



Cite this: *Environ. Sci.: Processes Impacts*, 2024, 26, 2051

## Exploring the interactions of glyphosate in soil: the sorption scenario upon soil depletion and effect on waterleaf (*Talinum triangulare*) growth

Paul N. Diagboya,<sup>a</sup> Bamidele I. Olu-Owolabi<sup>c</sup> and Rolf-Alexander Düring<sup>a</sup>

The pesticide glyphosate has contributed immensely to the ease of farming and high yields. However, the ever-increasing environmental input of pesticides is of particular interest due to several unintended effects on non-target organisms. In soil, the sorption, transport, possible uptake, and effect on plant growth are still not well understood, and much so for the sub-Saharan. Sorption processes are contingent on the soil composition, characteristics, and ambient conditions, and these are becoming increasingly affected by climate change in a way that may alter pesticide fate. Hence, representative sub-Saharan whole soil (WS) treated to eliminate organic matter (OMR) and iron oxides (IOR) was employed to ascertain the contributions of these major constituents to glyphosate sorption processes, as well as ascertain the effect of glyphosate in soil on the growth of *Talinum triangulare*–waterleaf. Glyphosate sorption for all treatments was rapid with equilibrium at around 720 min. The sorption decreased as pH increased, and was concentration-dependent, gradually increasing with glyphosate concentration. The process was endothermic, and sorption data were better described by the fractal pseudo-second-order and Freundlich adsorption isotherm models, suggesting a complex interplay of interactive sorption forces. The IOR sample (with iron oxide depleted but organic matter intact) exhibited higher sorption than the OMR and WS, highlighting the contribution of organic matter in glyphosate sorption. Hysteresis was high for all samples and increased with temperature. Considering the unregulated usage of glyphosate in the sub-Saharan, the poor sorption, especially in treated soils, observed in this study suggests a high possibility of glyphosate leaching into the aquifer and poisoning of this water source, while the high hysteresis implied the bio-availability of glyphosate in surface soil for plant absorption, hence affecting growth; as confirmed in the waterleaf growth study where growth in the organic-matter/iron-oxide-depleted soils was substantially stunted. Hence, glyphosate affects waterleaf growth, especially in organic-matter/iron-oxide-depleted soils.

Received 16th July 2024  
Accepted 26th September 2024

DOI: 10.1039/d4em00433g

rsc.li/epsi

### Environmental significance

Though pesticides have contributed immensely to agricultural productivity, the ever-increasing input of pesticides, such as glyphosate, into the environment is of particular interest due to several unintended effects. To remediate glyphosate in the environment, it is vital to understand its fate which is largely unknown especially in less studied sub-Saharan soils. This may be compounded by the increasing effect of climate change on the soil's properties which is believed to alter glyphosate fate. Thus, glyphosate sorption and desorption, and effect of glyphosate on plant growth were studied in sub-Saharan soil using a fast growing vegetable-*Talinum triangulare* (waterleaf). The soil was pre-treated to mimic some effects of climate-induced changes on its properties. This study found that glyphosate sorption was low and largely affected by soil properties which were altered by climate-induced factors, while waterleaf growth in the presence of glyphosate was heavily stunted especially in the climate affected soil.

## 1 Introduction

Agrochemicals, especially pesticides, have contributed immensely to the recent high agricultural yields. However, the increased usage and ever-increasing environmental inputs of pesticides make them of particular interest, and this is proving progressively problematic to the ecosystem and human health due to several unintended effects such as environmental contamination and toxicity to non-target organisms.<sup>1–4</sup> Some of

<sup>a</sup>Institute of Soil Science and Soil Conservation, Research Centre for BioSystems, Land Use and Nutrition (iFZ), Justus Liebig University Giessen, Heinrich-Buff-Ring 26, 35392 Giessen, Germany. E-mail: pauldn2@yahoo.com

<sup>b</sup>Environmental Fate of Chemicals and Remediation (EnFaCre) Laboratory, Department of Environmental Management and Toxicology, University of Delta, PMB 2090, Agbor, Nigeria

<sup>c</sup>Department of Chemistry, University of Ibadan, Ibadan, Nigeria



the associated effects include tissue and DNA damage, endocrine disruption, and carcinogenesis.<sup>5</sup> In the environment, their transport, effects, and fate are major focuses of interest.<sup>4,6,7</sup>

The fate of pesticides in the environment is mainly controlled by sorption processes in soils, and this affects the successive chemical reactivity and transport in aquatic systems, as well as the effects on plants.<sup>8</sup> Sorption processes are contingent on the composition, characteristics, and ambient conditions of soil, and these include the minerals and clay contents/types, soil organic matter (SOM), pH, and temperature.<sup>8–11</sup> Around the world, the effects of climate change are becoming increasingly obvious, and this is affecting soil properties in a way that may alter its pesticide sorption potential and the ultimate fate of pesticides. Some of these effects include depletion and/or erosion of topsoil constituents such as SOM and soil iron oxides (SIO) arising from higher soil temperatures and unprecedented flooding in several parts of the world.<sup>12,13</sup> With regards to pesticide sorption and fate, soil's response to these climate change-induced effects is not yet known, and more so for the less studied sub-Saharan soils. The sub-Saharan region is distinctive in that the region contributes very little to global climate change, but projections show that it will be disproportionately affected.<sup>14,15</sup> This projection is proving to be correct as the region, in 2022, reported the worst vegetation and farm crop wash-off, and topsoil erosion resulting from flooding.<sup>16–18</sup>

Apart from the ever-increasing global environmental inputs of pesticides, field observations show alarmingly high and unregulated usage of agricultural pesticides in the sub-Saharan region, and glyphosate is one of the major culprits in this regard.<sup>19–21</sup> Glyphosate is a strong chelating agent with three functional groups (amine, carboxylate, and phosphonate) and one of the most applied pesticides around the world. It is a non-selective and systemic post-emergent pesticide that obstructs the shikimate pathway in plants responsible for the synthesis of the essential aromatic amino acids that are precursors of benzoic acids, alkaloids, lignin, flavonoids, and vitamin K.<sup>19,20,22</sup> Recently, glyphosate and its metabolite, amino-methyl-phosphonic acid (AMPA), have been commonly detected in various environmental media, and this is causing serious concerns due to its effects on the ecosystem and humans especially.<sup>22–24</sup> This has led to the re-classification of glyphosate as a probable human carcinogen or category 2A carcinogen by the International Agency for Research on Cancer (IARC).<sup>25,26</sup>

Several studies have reported the fate of glyphosate in soils from different parts of the world,<sup>22,27–30</sup> and only one report was found for glyphosate sorption in sub-Saharan soil.<sup>31</sup> None of these studied the effect of climate-induced changes on the fate of glyphosate in soils or glyphosate uptake by edible plants. A study showed the uptake of glyphosate in weeds but not in edible plants—which is far more important in terms of food security.<sup>32</sup> The key point in the aforementioned literature is that the fates of pesticides, such as glyphosate, in climate change-induced depleted soils are unknown. Hence, the objective of the study was to eliminate major soil constituents (SOM and SIO) from a sub-Sahara obtained soil and use the treated and untreated samples for glyphosate sorption and desorption

study by examining the sorption rate, effects of pH, concentration, and temperature variations. The obtained data will be explained using various kinetics and adsorption isotherm models. A cursory 12-week study of the effect of glyphosate on *Talinum triangulare* (waterleaf) growth was also carried out on the treated and untreated soils spiked with known glyphosate concentrations. To the best of our knowledge, no such study on the effect of glyphosate on waterleaf has been carried out.

## 2 Experimental

### 2.1 Soil sampling and treatments

Randomized sub-Saharan topsoil samples (0–30 cm) obtained from Emuhu farming vicinity (6° 16' 57" N; 6° 16' 14" E), Nigeria, were used for the study. Heavy use of pesticides was observed in this location, like most farming areas in west Africa. The sample pretreatment included air drying, stone and dirt sorting, and sieving (1.0 mm sieve). Parts of the pretreated whole sample (WS) were used for the soil organic matter (SOM) and soil iron oxide (SIO) depletion treatments. Depletion of the SOM involved continuous 30% H<sub>2</sub>O<sub>2</sub> gradual treatment in a water bath set at 80 °C over 48 h until the frothing stopped. Excess frothing was lowered by the addition of cold water to avoid sample loss.<sup>33,34</sup> The sample was washed (7 times centrifugation at 3500 rpm), oven dried (40 °C for 48 h), and labeled OMR. The SIO depletion process employed 0.3 M Na-citrate (Sigma-Aldrich) solution (400 mL) and 1 M NaHCO<sub>3</sub> (Sigma-Aldrich) solution (50 mL) on 400 g of the WS in a water bath at 80 °C. Ten grams of Na<sub>2</sub>S<sub>2</sub>O<sub>4</sub> (Merck) was added while stirring. After 15 min, saturated NaCl (Carl Roth) solution (10 mL) and acetone (HiPerSolv Chromanorm, HPLC grade) (10 mL) were added. The setup was left for 24 h before washing and drying as above,<sup>35</sup> and the sample was labeled IOR. Characterization of the pre/post-treated samples (Table 1) included determination of soil pH,<sup>36</sup> SOM,<sup>37</sup> soil particle size,<sup>38</sup> carbonates,<sup>39</sup> and metals (Varian 720ES ICP OES).<sup>40</sup> Extraction and determination of glyphosate in the pristine soil sample showed no glyphosate contamination in the soil.

### 2.2 Generation of glyphosate sorption on soil data and data treatment

Glyphosate (Sigma-Aldrich) working solutions were prepared in a background electrolyte of 0.1 KCl (Carl Roth) and 100 mg L<sup>-1</sup> sodium azide (Carl Roth) as the biocide from a glyphosate stock solution (1000 mg L<sup>-1</sup> at 4 °C) made in water (Milli-Q; pH 7 ± 0.2). Typically, a replicate batch sorption study using 500 mg of soil sample in 20 mL glyphosate working solution of a specific concentration was carried out in a 20 mL amber glass vial mounted on an orbital shaker at 200 rpm for a specified time to equilibrate. At equilibrium, the vial was withdrawn, centrifuged (2000 rpm for 10 min), and filtered through a 0.45 µm PES syringe filter, before glyphosate quantification using a HPLC (Thermo Scientific) coupled to an MS (Thermo Scientific Exactive Orbitrap) detector (HPLC-MS). The resolution of the Orbitrap is very high such that an exact determination of the mass of the analyte is possible.



Table 1 Pre- and post-treated soil characteristics<sup>a</sup>

| Soil | pH (H <sub>2</sub> O) | SOM (%)     | CaCO <sub>3</sub> (%) | PSA (%) |       |      | Metals (mg kg <sup>-1</sup> ) |        |       |       |       |         |       |       |        |      |
|------|-----------------------|-------------|-----------------------|---------|-------|------|-------------------------------|--------|-------|-------|-------|---------|-------|-------|--------|------|
|      |                       |             |                       | *Sand   | *Silt | Clay | Fe                            | Na     | K     | Mg    | Ca    | Al      | Mn    | P     | S      | Zn   |
| WS   | 7.46                  | 2.08 ± 0.01 | 0.15                  | 87.6    | 5.7   | 6.7  | 18948.1                       | 21.5   | 184.1 | 391.5 | 825.6 | 16755.3 | 256.6 | 242.8 | 131.4  | 28.0 |
| OMR  | 5.86                  | 0.10 ± 0.19 | 0.17                  | 92.8    | 2.7   | 4.6  | 14277.8                       | 13.8   | 64.7  | 158.3 | 137.1 | 7543.7  | 77.8  | 136.8 | 54.5   | 10.8 |
| IOR  | 7.27                  | 1.66 ± 0.01 | 0.03                  | 86.5    | 4.5   | 9.0  | 5565.3                        | 2085.6 | 129.4 | 223.3 | 498.7 | 13127.9 | 52.7  | 160.2 | 1498.1 | 14.4 |

<sup>a</sup> \*PSA = Particle size analysis; \*% sand = sum of the coarse, medium, and fine sand; \*% silt = sum of the coarse, medium, and fine silt.

The WS, OMR, and IOR were employed for the sorption studies carried out at the natural soil pH using 26.6 mg L<sup>-1</sup> glyphosate solution at room temperature over 1440 min except otherwise stated. The following parameters were investigated: rate (over 1440 min), ambient solution pH (3–11), glyphosate concentration (7.3–46.4 mg L<sup>-1</sup>), and ambient temperature (22–42 °C). The solution pH value was regulated using 0.1 M NaOH or HCl. The glyphosate desorption study was carried out after the equilibrium experiment by cautiously decanting the equilibrium solution in each vial, refilling with a solution of the background electrolyte (and the biocide) but without glyphosate, and incubating the vial as in the equilibrium experiment. The solutions in the vials were subsequently centrifuged, and desorbed glyphosate was determined.

The quantification of glyphosate was carried out on an HPLC-MS using a slight modification of a reported protocol.<sup>41</sup> A Thermo Scientific 600 Pump with a Waters X-Bridge C18 3.5 μm column (150 mm × 2.1 mm inner diameter) at 27 °C was used for the chromatographic separation. The mobile phases A and B were 5 mM ammonium acetate (Carl Roth) and methanol (HiPerSolv Chromanorm, HPLC gradient), respectively, while the 5 min separation time followed a gradient program of 0–30 s, 90 : 10 (A : B); 30–90 s, 5 : 95 (A : B); 90–100 s, 0 : 100 (A : B); 100–200 s, 0 : 100 (A : B); and 200–300 s, 90 : 10 (A : B). A 10.0 μL injection volume and 300 μL min<sup>-1</sup> flow rate were employed,

with the equipment in negative ion mode and a scan mass range of 50–450 *m/z*. The HPLC was coupled to a high-resolution MS (Thermo Scientific Exactive Orbitrap). The Thermo Xcalibur Roadmap™ software was used to acquire the data and the quantitation was carried out by monitoring the primary transitions at an *m/z* of 168 and 110 for glyphosate and AMPA, respectively. The glyphosate calibration curve linear range (*r*<sup>2</sup> = 0.997) was obtained for ten concentrations between 0.05 and 25.0 mg L<sup>-1</sup> in aqueous 0.1 KCl. The limits of glyphosate detection and quantification were 5 and 50 ng L<sup>-1</sup> in water, respectively. Blank runs having no soil matrices were used to evaluate adsorption on walls and caps of the vials which were observed to be insubstantial.

The amounts (*q<sub>e</sub>*) of glyphosate adsorbed (mg g<sup>-1</sup>) were determined from the initial glyphosate concentrations (*C<sub>o</sub>*, mg L<sup>-1</sup>), equilibrium glyphosate concentrations (*C<sub>e</sub>*, mg L<sup>-1</sup>), soil mass (mg), and glyphosate volume (mL) by using eqn (1). Further analysis and description of the rate and equilibrium sorption data have been carried out using kinetics and equilibrium adsorption isotherm models, as well as thermodynamics variables (Tables 2–4). OriginPro 2015 (Origin Lab Corporation, USA) was employed in fitting the data.

$$q_e = (C_o - C_e)v/m \quad (1)$$

Table 2 Glyphosate adsorption kinetics model parameters

| Model of kinetics   | Parameter               | Parameter                                       | WS                   | OMR                  | IOR                  |
|---|-------------------------|---|----------------------|----------------------|----------------------|
| Pseudo-first-order (PFO);<br>$q_t = q_e(1 - e^{-k_1 t})$                                    | Sorption at equilibrium | $q_e$ (μg g <sup>-1</sup> )                     | 0.23                 | 0.26                 | 0.30                 |
|   | Rate constant           | $k_1$ (min <sup>-1</sup> )                      | 0.77                 | 1.02                 | 0.97                 |
|   | Correlation coefficient | $r^2$   | 0.525                | 0.129                | 0.352                |
|   | Chi-square              | $\chi^2$  | $9.7 \times 10^{-4}$ | $3.5 \times 10^{-3}$ | $2.2 \times 10^{-3}$ |
| Pseudo-second-order (PSO);<br>$q_t = \frac{q_e^2 k_2 t}{1 + q_e k_2 t}$                     | Sorption at equilibrium | $q_e$ (μg g <sup>-1</sup> )                     | 0.23                 | 0.26                 | 0.31                 |
|   | Rate constant           | $k_2$ (g μg <sup>-1</sup> min <sup>-1</sup> )   | 3.65                 | 4.81                 | 3.92                 |
|   | Correlation coefficient | $r^2$   | 0.652                | 0.205                | 0.465                |
|   | Chi-square              | $\chi^2$  | $7.1 \times 10^{-4}$ | $3.2 \times 10^{-3}$ | $1.8 \times 10^{-3}$ |
| Fractal pseudo-second-order (FPSO); $q_t = \frac{k_f q_e^2 t^\alpha}{1 + k_f q_e t^\alpha}$ | Sorption at equilibrium | $q_e$ (μg g <sup>-1</sup> )                     | 0.35                 | 17.36                | 2.83                 |
|   | Rate constant           | $k_f$   | 1.54                 | $4.5 \times 10^{-4}$ | $2.4 \times 10^{-2}$ |
|   | Fractional time index   | $\alpha$  | 0.23                 | 0.12                 | 0.10                 |
|   | Correlation coefficient | $r^2$   | 0.969                | 0.844                | 0.969                |
| Intra-particle-diffusion (IPD);<br>$q_e = k_{IPD} t^{1/2} + C$                              | Chi-square              | $\chi^2$  | $6.4 \times 10^{-5}$ | $6.2 \times 10^{-4}$ | $1.1 \times 10^{-4}$ |
|   | Surface sorption        | $C$ (μg g <sup>-1</sup> )                       | 0.16                 | 0.17                 | 0.22                 |
|   | Rate constant           | $k_i$ (g μg <sup>-1</sup> min <sup>-1/2</sup> ) | $3.3 \times 10^{-3}$ | $5.1 \times 10^{-3}$ | $4.4 \times 10^{-3}$ |
|   | Correlation coefficient | $r^2$   | 0.741                | 0.978                | 0.845                |
| Experimental  | Chi-square              | $\chi^2$  | $5.3 \times 10^{-4}$ | $8.9 \times 10^{-5}$ | $5.3 \times 10^{-4}$ |
|   |                         | $q_e$ (μg g <sup>-1</sup> )                     | 0.27                 | 0.37                 | 0.37                 |



Table 3 Thermodynamics variables for glyphosate sorption

| Parameter   | WS       | OMR    | IOR   |
|---|----------|--------|-------|
| $\Delta H^\circ$ (kJ mol <sup>-1</sup> )                | 5.30     | 0.74   | 13.81 |
| $\Delta S^\circ$ (J mol <sup>-1</sup> K <sup>-1</sup> ) | -6.87    | -24.67 | 24.90 |
| $\Delta G^\circ$ (kJ mol <sup>-1</sup> )                | 288.15 K | 7.66   | 7.83  |
|   | 298.15 K | 6.67   | 8.65  |
|   | 307.15 K | 7.85   | 8.30  |

### 2.3 Effect of glyphosate on plant growth in climate-impacted soil

The study of the effect of glyphosate on *Talinum triangulare* (waterleaf) growth in the climate-impacted soil was carried out by spiking the WS, OMR, and IOR soils with environmentally feasible glyphosate concentrations of 460 and 230  $\mu\text{g kg}^{-1}$  soil, which are within the recommended use rates of 0.22 and 1.7 kg ha<sup>-1</sup>, and assuming that field dissipation is within 5 cm of the topsoil.<sup>42,43</sup> The spiked soils were then aged for 3 weeks before planting 10 replicates, while the time between germination and harvesting was six (6) weeks. The growth experiment was carried out in a climate chamber with 13 h daylight at 30 °C, 75% light intensity, 11 h darkness at 24 °C, and 60% relative humidity. The fertilizer (NPK: Nitrogen-12%; P<sub>2</sub>O<sub>5</sub>-12%; Potassium-17%; Manganese-2%) was added to aid plant growth in soils at a rate of 2 g to 0.9 kg soil.

## 3 Results and discussion

### 3.1 Description of experimental soil

Granulometric analysis of the WS (Table 1) showed that the pristine soil has a high sand fraction (87.6%) with a low silt content (5.7%); high sand content may be typical of most sub-Saharan soils.<sup>44,45</sup> The characterization data (Table 1) also showed mutual relationships between the treatments and the amounts of SOM and SIO in each sample; for instance, the OMR sample lost  $\approx 94\%$  of its inherent SOM compared to the IOR sample which lost  $\approx 21\%$  SOM during the H<sub>2</sub>O<sub>2</sub> treatment. Similarly, during the dithionite treatment, the IOR sample lost

$\approx 71\%$  of its inherent iron content compared to the OMR which lost  $\approx 25\%$ . Thus compared to the WS sample, OMR and IOR retained  $\approx 6$  and 79% of the inherent SOM, respectively, with  $\approx 75$  and 29% inherent soil iron, accordingly. A substantial quantity ( $\geq 50\%$ ) of the SOM is associated with the silt fraction in the WS which resulted in a loss of about half of the silt fraction in the WS upon SOM removal in the OMR sample. The reportedly high iron oxide (gibbsite, goethite, and hematite) contents of Sub-Saharan soils could be a plausible reason for the non-complete destruction of organic matter because these oxides form stable organo-mineral complexes with SOM. This leads to chemical protection of the organic matter and limits the H<sub>2</sub>O<sub>2</sub> efficiency to oxidize the SOM.<sup>9,10,34</sup> A similar form of chemical protection may be responsible for the non-complete destruction of the iron oxides following the dithionite treatment.

In the presence of organic matter both in the WS and IOR samples, the soil exhibited an almost neutral pH in water with a slight tendency towards alkalinity. Upon organic matter removal in the OMR, the soil expressed an acidic pH in water. Thus, the presence of SOM in this soil helps maintain soil pH neutrality, while the soil iron oxides with lower organic matter content drive the pH towards acidic values; this trend may be peculiar to sub-Saharan soils.<sup>33</sup>

Another major observation is the metal contents after various treatments: upon removal of organic matter (in OMR), there were substantial ( $\geq 50\%$ ) losses of the inherent Na, K, Mg, Ca, and Al contents which are vital metals for soil cation exchange capacity. However, Na and S expressed exponential increases upon iron oxide removal in the IOR sample. These observations could be a unique feature of sub-Saharan soils since similar results were observed for some soils from this region<sup>34</sup> and may be ascribed to the unmasking of inherent Na<sup>+</sup> ions and sulphur within soil components like minerals, clays, and SOM after iron oxide removal.

### 3.2 Glyphosate kinetics and pH studies

The rate trends for glyphosate sorption on the WS, OMR, and IOR samples were observed over 1440 min (Fig. 1a). This

Table 4 Glyphosate adsorption isotherm model variables at 42 °C (temperature of highest sorption)

| Adsorption isotherm  | Parameter                     | Parameter                        | WS@42 °C             | OMR@42 °C            | IOR@42 °C            |
|--|-------------------------------|----------------------------------|----------------------|----------------------|----------------------|
| Langmuir model; $q_e = \frac{Q_o b C_e}{1 + b C_e}$  | Sorption capacity             | $Q_o$ (mg g <sup>-1</sup> )      | 0.405                | 0.487                | 0.547                |
|  | Energy-related factor         | $b$                              | 0.102                | 0.075                | 0.191                |
|  | Correlation coefficient       | $r^2$                            | 0.899                | 0.922                | 0.927                |
|  | Chi-square                    | $\chi^2$                         | $8.1 \times 10^{-4}$ | $8.1 \times 10^{-4}$ | $1.4 \times 10^{-3}$ |
| Freundlich model; $q_e = k_f C_e^n$  | Freundlich constant           | $k_f$                            | 0.065                | 0.058                | 0.120                |
|  | Freundlich linearity constant | $n$                              | 0.468                | 0.528                | 0.438                |
|  | Correlation coefficient       | $r^2$                            | 0.968                | 0.956                | 0.957                |
|  | Chi-square                    | $\chi^2$                         | $2.6 \times 10^{-4}$ | $4.6 \times 10^{-4}$ | $8.6 \times 10^{-4}$ |
| Langmuir-Freundlich (L-F) model; $q_e = \frac{Q_{\max}(K_{LF} C_e)^n}{1 + (K_{LF} C_e)^n}$ | Sorption capacity             | $Q_{\max}$ (mg g <sup>-1</sup> ) | 55.60                | 38.17                | 21.20                |
|  | L-F constant                  | $K_{LF}$                         | $1.2 \times 10^{-3}$ | $1.5 \times 10^{-3}$ | $5.7 \times 10^{-3}$ |
|  | L-F linearity constant        | $n$                              | 0.470                | 0.531                | 0.444                |
|  | Correlation coefficient       | $r^2$                            | 0.952                | 0.933                | 0.935                |
| Experimental   | Chi-square                    | $\chi^2$                         | $3.9 \times 10^{-4}$ | $6.9 \times 10^{-4}$ | $1.3 \times 10^{-3}$ |
|  |                               | $q_e$ (mg g <sup>-1</sup> )      | 0.33                 | 0.36                 | 0.49                 |



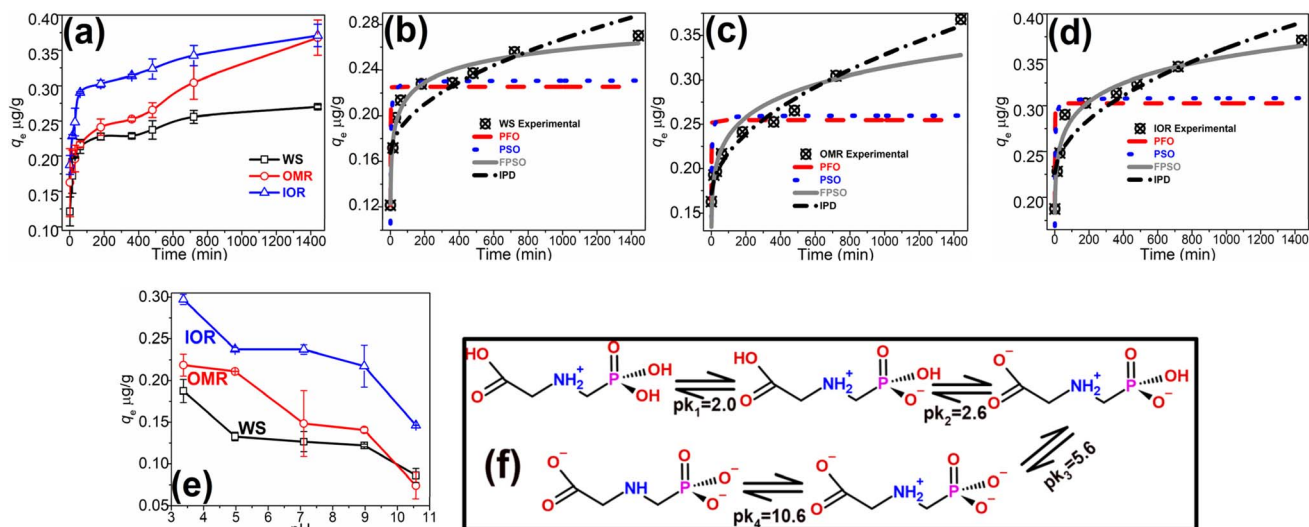


Fig. 1 (a) Glyphosate sorption rate trends in the soils; comparison of rate data fittings by the kinetics models for (b) WS, (c) OMR, and (d) IOR soils; (e) sorption trends at varying solution pH; and (f) glyphosate ionization at varying pH.

enabled the prediction of the time for each soil to attain equilibrium glyphosate sorption, as well as the mechanism of glyphosate uptake. The trends showed a rapid glyphosate uptake on the numerous unoccupied sorption sites within the first 60 min of the sorption commencement (at this point  $\geq 81\%$  of total sorption occurred for the WS and IOR, and  $\approx 66\%$  for OMR), and subsequently, a slower uptake towards equilibrium represented by the steady rise in the curve in Fig. 1a until the rise was insubstantial marking the time of equilibrium attainment. For all samples, the equilibrium was observed at about 720 min and there was no relative difference in equilibrium attainment time:  $WS_{720 \text{ min}} = IOR_{720 \text{ min}} = OMR_{720 \text{ min}}$ ; however, 1440 min was employed for subsequent experiments. Regardless of the similar equilibrium time, differences were observed in the amount of glyphosate uptake by each treatment, highlighting the contributions of the soil components in the sorption process. In this regard, the sorption trend was  $IOR > OMR > WS$ .

The variation in sorption may be attributed to the relative interaction between the structure of glyphosate (Fig. 1f) and the exposed soils' surfaces of each treatment. In the OMR sample, SOM removal resulted in the exposure of charged non-aromatic (non-humic) mineral surfaces (especially due to the high content of iron oxides, such as gibbsite, haematite, and goethite, in sub-Saharan soils<sup>34</sup>), while iron oxide removal in the IOR sample exposed several aromatic and humic materials with various charged functional groups. These are the surface sites that interact with glyphosate to varying degrees, in addition to the presence of soil pores where glyphosate molecules could be "trapped" during sorption. Irrespective of the charge type exposed in the soil, glyphosate is bi-charged and can form electrostatic interaction leading to its adsorption. Though the WS has a full aggregate of inherent iron oxides and organic matter, the relatively lower sorption observed could be attributed to the chemical protection of some of the soil components

arising from stable organo-mineral complexes formed with SOM.<sup>10</sup> This results in the unavailability/blockage of some of these charged sorption surfaces, and hence lower sorption in the WS sample compared to the IOR soil.

The glyphosate sorption rate data for various treatments have been described by using four non-linear kinetics models (Table 2) to obtain some insights into the mechanisms of the sorption process. The models employed are the pseudo-first-order (PFO),<sup>46</sup> pseudo-second-order (PSO),<sup>46</sup> fractal pseudo-second-order (FPSO),<sup>47</sup> and intra-particle diffusion (IPD)<sup>48</sup> models. Their mathematical representations, the meaning of each parameter, and the non-linear plots' correlation coefficients ( $r^2$ ) and chi-square ( $\chi^2$ ) values are presented in Table 2, while the fittings are shown in Fig. 1b–d. The PFO model describes a very fast sorption process occurring within a few minutes of starting the process,<sup>46</sup> while the PSO model implies sorption involving the sharing or exchange of electrons between the adsorbent and contaminant.<sup>46,49</sup> On the other hand, the FPSO model involves more complex mechanisms likely comprising both mechanisms for the PFO and PSO models, and others.<sup>47,50</sup> The nearness of the  $r^2$  value to unity, the smaller  $\chi^2$  value, and a high correlation between the model estimated  $q_e$  and the experimentally obtained  $q_e$  value were used to determine the appropriateness of a model. Hence, the values of the  $r^2$ ,  $\chi^2$ , and  $q_e$  in Table 2 show that the rate data for all treatments fitted better to the FPSO model, and the process may be described by using this model. The model suggests a complex glyphosate sorption process involving an initial fast sorption within the first 60 min (Fig. 2a) and then a more gradual process later. Overall, the uptake process comprises electrostatic interaction involving the sharing or exchange of electrons, and possibly multi-layer sorption.

The IPD model (Fig. 1b–d) showed good fits for the data and exhibited comparatively high  $r^2$  ( $\geq 0.741$ ) and low  $\chi^2$  ( $\leq 5.3 \times 10^{-4}$ ) values. A dual-segment process was expressed by this



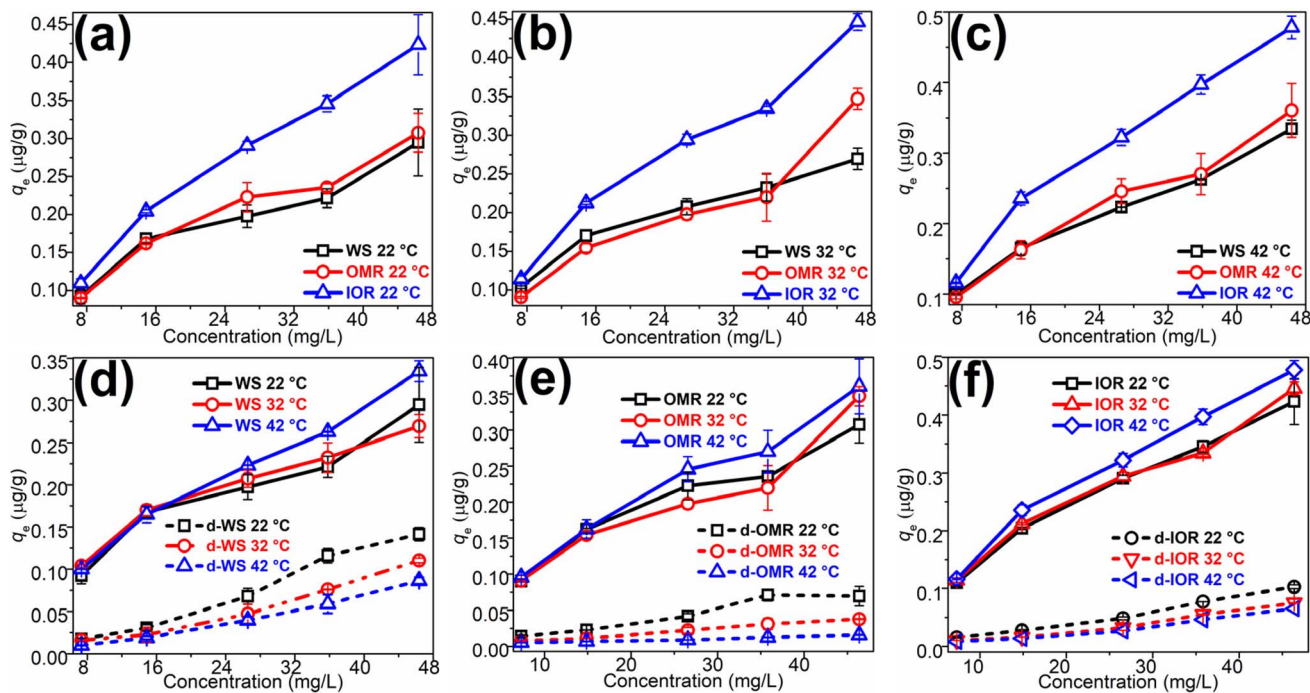


Fig. 2 Equilibrium sorption trends for the WS and treated soils at (a) 22 °C, (b) 32 °C, and (c) 42 °C; comparison of sorption and desorption trends at varying temperatures for the (d) WS, (e) OMR, and (f) IOR soils.

model, representing an initial fast sorption controlled by boundary layer diffusion of glyphosate molecules from solutions across the soils' external surfaces, followed by a later slower stage controlled by intra-particle diffusion of glyphosate molecules within soil phases. Thus, no one mechanism dominated the sorption process, and this was also confirmed by the model curves not passing through the plots' origins.<sup>50,51</sup> The estimated surface sorption,  $C$ , values of the model indicated that  $\approx 59\%$  of the glyphosate sorption process was a surface phenomenon on the WS and IOR, while it was 46% on the OMR sample.

The response to changes in ambient environment pH is one important factor that determines the trend and degree of sorption of any particular contaminant because pH influences the soil's charge density, hence affecting its response to the presence of aqueous contaminant(s), as well as a contaminant's speciation, and ultimately the sorption process.<sup>33,52</sup> Thus, the effect of soil pH on glyphosate sorption has been tested within a pH range of 3 and 11 as depicted in Fig. 1e. The highest glyphosate sorption was observed in the acidic region (at  $\approx \text{pH}$  3); the trend showed decreasing sorption as pH increased, an observation consistent with some literature reports.<sup>20,53</sup> This supports the assertion that the interaction between the soil (which is rich in positive and negatively charged surfaces) and glyphosate is mainly electrostatic, and may be attributed to changes in soils and glyphosate ionizations at varying pH. For instance, the glyphosate molecule has a central amine group sandwiched between carboxylic and phosphate functional groups (Fig. 1f); this amine group is positively charged between pH 2 and 5.6, while only one of the three oxygen atoms of the

phosphate group is deprotonated (negatively charged) in this pH range.<sup>53</sup> This is a perfect recipe for electrostatic attraction between oppositely charged soil surfaces, and thus, the observed high sorption. However as pH increases from 2, the amine group and two of the three phosphate oxygen atoms are gradually deprotonated (Fig. 1f), and the glyphosate molecule becomes progressively negatively charged, lowering the possibility of electrostatic interaction, hence leading to the continuously lower sorption recorded. In addition to sorption *via* electrostatic interaction between glyphosate and the charged soil sites, there is the plausibility of hydrogen bonding, as well as further electrostatic interactions between surface-adsorbed glyphosate and glyphosate in solution resulting in multi-layer adsorption – this theory was tested by fitting various adsorption isotherm models to the experimental data.

### 3.3 Glyphosate sorption: equilibrium studies

Equilibrium sorption trends of various soil treatments using a glyphosate concentration range of 5–40  $\text{mg L}^{-1}$  at temperatures between 22 and 42 °C are depicted in Fig. 2a–f. Overall, the trends are concentration-dependent, and a gradual rise in glyphosate sorption was observed as the initial solution concentration was moderately increased; a trend consistent with the literature.<sup>4,20</sup> This trend may be ascribed to two factors: a possible transfer of glyphosate molecules from saturated soil surface boundaries to the constituents' phases or into pores as the solution concentration increased,<sup>54</sup> as well as the plausible formation of multi-layer films *via* electrostatic interactions between surface adsorbed glyphosate and glyphosate in solution<sup>55</sup> as proposed earlier.



A comparative evaluation of the sorbed quantities by the various treatments (Fig. 2a–c) showed that within the studied temperature range, the IOR sample exhibited higher glyphosate sorption than the whole soil or the OMR with the trend – IOR > WS  $\approx$  OMR. This suggests that SOM in this soil contributed more ( $\approx 25\%$ ) to glyphosate sorption than other components.<sup>27</sup> It seemed that the co-presence of SOM and iron oxides in the WS did not substantially influence the sorption process because the vital SOM-associated-sorption sites might have been masked by chemical protection *via* the formation of stable organo–mineral complexes<sup>10</sup> resulting in lower sorption.

Similarly, a comparison of glyphosate sorption by each treatment but at varying temperatures (Fig. 2d–f) showed that sorption was favoured at higher temperatures –  $42 > 32 \geq 22$  °C, suggesting that irrespective of the treatment, the process was somewhat endothermic. This assumption was then examined by calculating the thermodynamics parameters which are presented in Table 3 and described briefly. The  $\Delta H^\circ$  values, which were positive, confirmed the endothermic nature of the process, and thus higher temperatures within the range of this study would enhance glyphosate sorption. In alignment with this result, the positive  $\Delta G^\circ$  values suggest that the input of external heat energy is needed to facilitate the transfer of aqueous glyphosate from the solution to the bulk phase, while the values of  $\Delta S^\circ$  indicated decreased entropy of glyphosate molecules at the soil–solution boundary as the process approached equilibrium. The very low  $\Delta H^\circ$  values ( $\leq 20$  kJ mol<sup>-1</sup>) are an indication that the process involved weak forces of attraction such as electrostatic interaction and hydrogen bonding.<sup>55,56</sup>

Glyphosate desorption from all soil treatments and at varying temperatures was evaluated after a single desorption step at 1440 min, and the trends are presented in Fig. 2d–f. It was observed that there was  $\approx 52\%$  hysteresis for the WS at 22 °C, expressing the highest glyphosate desorption ( $\approx 48\%$ ). At higher temperatures, hysteresis increased to  $\approx 59\%$  (32 °C) and 74% (42 °C) for the WS resulting in lower desorption values of 41 and 26%, respectively. The desorption percentages were lower (higher hysteresis) at 22, 32, and 42 °C for the OMR (22.6, 10.9, and 4.4%) and IOR (24.3, 16.9, and 13.7%) treated soils, respectively, suggesting that the exposed surfaces of the treated soils bond the glyphosate molecules more than on the WS soil. Over the entire temperature range studied, the average

glyphosate desorption for WS, OMR, and IOR was 38.2, 12.7, and 18.3%, respectively. This suggests that the soil treatments that involved the breakdown of the soil organo–mineral complexes exposed sorption surfaces that bind glyphosate strongly compared to sorption sites on the WS, resulting in lower desorption or higher hysteresis in the OMR and IOR samples. Additionally, the low desorption from this soil could be a result of a relatively high glyphosate amount being ‘trapped’ within soil phases as indicated by the IPD model. Considering the unregulated usage of glyphosate in the sub-Saharan, the poor glyphosate sorption observed in this study could mean that there is a possibility of glyphosate leaching into the aquifer and poisoning this water source. Additionally, the relatively high hysteresis may imply the availability of glyphosate for plant uptake on surface soils, resulting in bio-accumulation or even growth stunting.

Glyphosate equilibrium sorption data for the various treatments obtained at 42 °C were fitted with three adsorption isotherm models (Langmuir,<sup>57</sup> Freundlich,<sup>58</sup> and Langmuir–Freundlich<sup>59</sup>) to predict the mechanism(s) involved in glyphosate sorption in these samples. The mathematical representations of these models, the model parameters,  $r^2$ , and  $\chi^2$  values are detailed in Table 4, and the fittings are presented in Fig. 3a–c. As in the kinetics model, the  $r^2$ , and  $\chi^2$  values were used to determine the appropriateness of each model. A comparative evaluation of the models using the fittings (Fig. 3a–c) and model parameters (Table 4), especially the  $r^2$  ( $\geq 0.956$ ) and  $\chi^2$  ( $\leq 8.6 \times 10^{-4}$ ) values, showed that the Freundlich model fitted the data better. This suggests that glyphosate sorption occurred at non-identical sorption sites that were energetically distinct from each other and there was the possibility of multi-layer adsorption<sup>58</sup> considering the heterogeneous nature of soils and the different ionizations of glyphosate (Fig. 1f). The implication of the Freundlich model opposed that of the Langmuir model which suggests monolayer glyphosate sorption occurring at finite, structurally, and energetically similar soil sites.<sup>57</sup> The Langmuir–Freundlich model is a combination of both models;<sup>59</sup> though it fits the data ( $r^2 \geq 0.933$ ;  $\chi^2 \leq 1.3 \times 10^{-3}$ ) better than the Langmuir model and could be used to explain the sorption, the Freundlich model is still better at describing the glyphosate sorption process. The Freundlich and Langmuir–Freundlich models’ non-linearity constants  $n$  were less

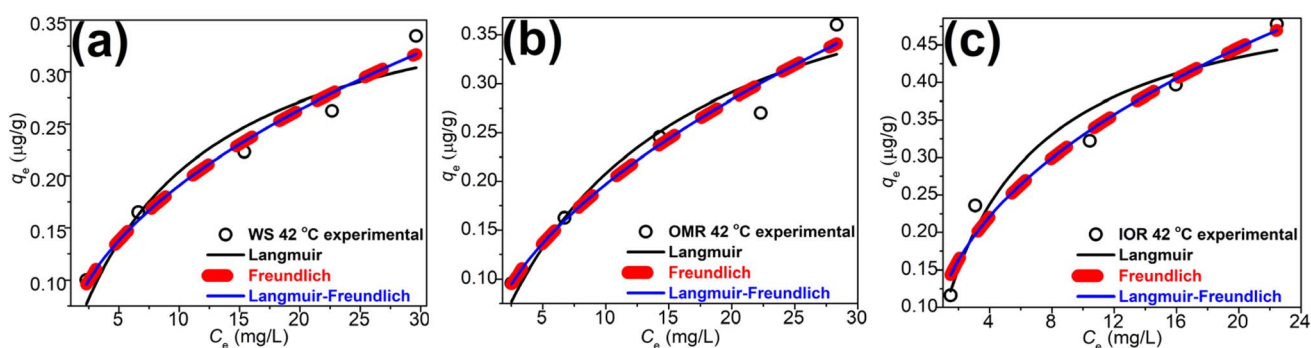


Fig. 3 Equilibrium data fittings to the Langmuir, Freundlich, and Langmuir–Freundlich adsorption isotherm models for (a) WS, (b) OMR, and (c) IOR soils.



than unity ( $\leq 0.531$ ) indicating that at higher glyphosate concentrations, the sorption tends towards non-linearity. In summary, the kinetics and adsorption isotherm models suggested a complex interplay of interactive sorption forces in glyphosate uptake composed mainly of electrostatic interactions, hydrogen bonding, and multi-layer adsorption.

### 3.4 Effect of glyphosate on waterleaf growth in climate-impacted soil

The soil treatments were incubated for 21 days after spiking with environmentally applicably glyphosate concentrations of 230 and 460  $\mu\text{g kg}^{-1}$  (which are within the field application range of 0.84–1.7  $\text{kg ha}^{-1}$  (ref. 42)), as well as a very high concentration of 1000  $\mu\text{g kg}^{-1}$ . The waterleaf plants were grown for 6 weeks before harvesting. The grown waterleaf plants and the percent loss in vegetative parts are presented in Fig. 4 and 5, respectively. As shown in Fig. 5, the recorded growth in the control was taken as the full growth potential or 100% (within the experimental condition) while the recorded growth values in the treatments were compared to this value. The results showed that the waterleaf in the control pots (WS sample without glyphosate) exhibited excellent growth with plenty of vegetative parts. However, the WS samples containing glyphosate expressed increasingly lower vegetative growth with increasing soil glyphosate concentration (Fig. 4a and 5). There were easily observable growth differences as the glyphosate concentrations increased in the WS samples. A vegetative loss of about 12% was observed in the 230  $\mu\text{g kg}^{-1}$  treatment with higher losses of  $\approx 52$  and 87% at 460 and 1000  $\mu\text{g kg}^{-1}$ , respectively. This is a clear indication that the applied glyphosate in the untreated soil affected waterleaf vegetation production.

Similarly, the presence of glyphosate concentrations which are within the field application range in the treated soils with depleted inherent soil constituents (SOM and iron oxides) resulted in substantially lower growth of waterleaf compared to



Fig. 5 Percentage of mass loss of vegetative parts for all soil treatments.

the WS samples (Fig. 4b and 5). The growth reduction was more severe in the iron oxide-depleted soil samples (IOR) resulting in about 99% losses in the vegetative parts compared to the loss in the OMR samples ( $\approx 94\%$ ). The vegetation losses in the treated samples were both very high, and this trend may be due to the higher glyphosate sorption and ease of desorption by these treatments, making glyphosate easily bio-available leading to growth inhibition. A possible reason for the slightly better waterleaf growth in the organic matter-depleted soils (OMR soils) could be that since iron oxides adsorb less glyphosate (as seen from experimental data), during irrigation glyphosate may seep freely to the sub-surface soil away from the plant's roots resulting in less interaction with glyphosate and lowered effect on growth.

Overall, the WS samples with/without glyphosate exhibited better waterleaf growth than the treatments, but it was established that glyphosate in soil affects waterleaf growth. Though this is a cursory lab-scale study and the use of a more realistic mesocosm study is recommended, it does however indicate that the presence of pesticides such as glyphosate in organic matter/iron-oxide-depleted-soils may affect plant (waterleaf) growth and ultimately result in bio-accumulation.

## 4 Conclusion

The impact of major soil constituents on glyphosate sorption by sub-Saharan soil with varying treatments (whole soil-WS, substantially depleted organic matter (OMR), and iron oxides (IOR)) was studied, as well as the effect of glyphosate in these soils on waterleaf growth. Upon treatment, the almost neutral pH of the WS and IOR soils were not substantially changed, unlike the OMR soil which became slightly acidic. Substantial amounts ( $\geq 50\%$ ) of essential plant micronutrients and inherent exchangeable cations (Na, K, Mg, Ca, and Al) were lost upon organic matter depletion, but the iron oxide depletion resulted in an exponential rise in the quantities of Na and sulphur. Glyphosate sorption decreases at higher pH and is concentration-dependent, gradually increasing with glyphosate concentration. The equilibrium in all treatments was attained

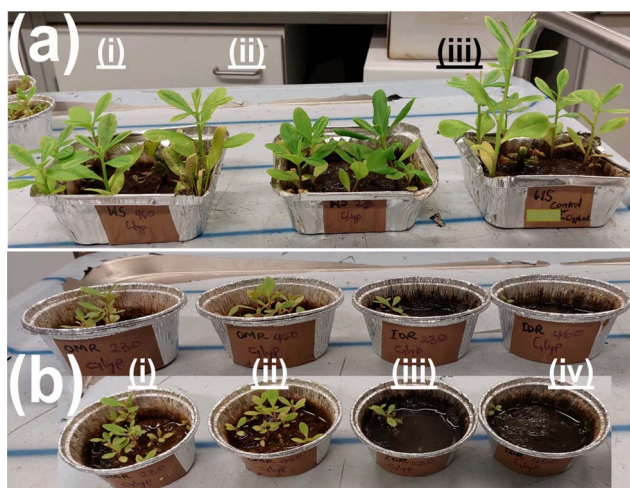


Fig. 4 Effect of glyphosate in soil on waterleaf growth in (a) (i) WS-460, (ii) WS-230, (iii) WS control; (b) OMR and IOR (i) OMR-230, (ii) OMR-460, (iii) IOR-230, and (iv) IOR-460 (number on the soil treatment indicates the glyphosate concentration in  $\mu\text{g kg}^{-1}$ ).



at around 720 min. The process was endothermic and could be best explained by the fractal pseudo-second-order and Freundlich adsorption isotherm models, implying a complex interplay of interactive sorption forces composed mainly of electrostatic interactions, hydrogen bonding, and multi-layer adsorption, as well as 'trapping' within the soil phases. The IOR soil exhibited higher sorption than treatments (IOR > WS  $\geq$  OMR), highlighting the contribution of SOM ( $\approx 25\%$ ) in glyphosate sorption. In the unperturbed WS with a full aggregate of inherent iron oxides and SOM, chemical protection of the sorption sites within the iron oxides and organic matter components arising from the formation of stable organo-mineral complexes resulted in slightly lower sorption. Hysteresis was high for all samples and increased with temperature. Considering the unregulated usage of glyphosate in the sub-Saharan, the glyphosate sorption trends observed in this study suggest the possibility of glyphosate leaching into the aquifer, while the relatively high hysteresis implies the bio-availability of glyphosate in surface soil for plant absorption, hence affecting growth. The latter theory was confirmed in the waterleaf growth study where growth in the unperturbed whole soil was less affected unlike in the organic-matter/iron-oxide-depleted soils where it was substantially stunted. Hence, glyphosate affects waterleaf growth, especially in organic-matter/iron-oxide-depleted soils.

## Ethical approval and consent to participate

We declare that we have no human participants or data.

## Data availability

The datasets used and analyzed during the current study are available upon request.

## Author contributions

P. N. Diagboya: conceptualization, formal analysis, funding acquisition, investigation, methodology, project administration, resources, validation, writing – original draft; B. I. Olu-Owolabi: conceptualization, methodology, project administration, validation, writing -review & editing; R.-A. Düring: formal analysis, funding acquisition, investigation, methodology, project administration, resources, supervision, validation, writing – review & editing. All authors have approved and contributed to the final manuscript.

## Conflicts of interest

The authors have no relevant financial or non-financial interests to disclose.

## Acknowledgements

We acknowledge the support of the Alexander von Humboldt Foundation, Germany, for providing the funding for this study, as well as Elke Müller (Justus Liebig University-JLU), Elke

Schneidenwind (JLU), and Benjamin J. Heyde (JLU) for their technical assistance.

## References

- 1 M. W. Aktar, D. Sengupta and A. Chowdhury, Impact of pesticides use in agriculture: their benefits and hazards, *Interdiscip. Toxicol.*, 2009, **2**, 1–12.
- 2 F. N. Mtunzi, P. N. Diagboya, R.-A. Düring and B. I. Olu-Owolabi, Mesoporous SBA-15 Functionalized with G-5 Polyamidoamine: A Sustainable Adsorbent for Effective Sequestration of an Emerging Aqueous Contaminant, *ACS Appl. Nano Mater.*, 2021, **4**, 3052–3061.
- 3 J. Wilkinson, P. S. Hooda, J. Barker, S. Barton and J. Swinden, Occurrence, fate and transformation of emerging contaminants in water: An overarching review of the field, *Environ. Pollut.*, 2017, **231**, 954–970.
- 4 P. N. Diagboya, B. J. Heyde and R.-A. Düring, Efficient decontamination of aqueous glyphosate using Santa Barbara Amorphous-15 (SBA-15) and graphene oxide-SBA-15 poly-amidoamine functionalized composites, *Chem. Eng. J.*, 2023, 143263, DOI: [10.1016/j.cej.2023.143263](https://doi.org/10.1016/j.cej.2023.143263).
- 5 O. D. Ogunbiyi, D. O. Akamo, E. E. Oluwasanmi, J. Adebajo, B. A. Isafiade, T. J. Ogunbiyi, Y. A. Alli, D. T. Ayodele and P. O. Oladoye, Glyphosate-based herbicide: Impacts, detection, and removal strategies in environmental samples, *Groundw. Sustain. Dev.*, 2023, **22**, 100961.
- 6 A. Maddalon, V. Galbiati, C. Colosio, S. Mandić-Rajčević and E. Corsini, Glyphosate-based herbicides: Evidence of immune-endocrine alteration, *Toxicology*, 2021, **459**, 152851.
- 7 O. M. Strilbyska, S. A. Tsiumpala, I. I. Kozachyshyn, T. Strutynska, N. Burdyliuk, V. I. Lushchak and O. Lushchak, The effects of low-toxic herbicide Roundup and glyphosate on mitochondria, *EXCLI J.*, 2022, **21**, 183–196.
- 8 B. I. Olu-Owolabi, P. N. Diagboya and K. O. Adebawale, Evaluation of pyrene sorption-desorption on tropical soils, *J. Environ. Manage.*, 2014, **137**, 1–9.
- 9 E. C. Martins, V. de Freitas Melo, J. B. Bohone and G. Abate, Sorption and desorption of atrazine on soils: The effect of different soil fractions, *Geoderma*, 2018, **322**, 131–139.
- 10 B. Prado, C. Duwig, C. Hidalgo, K. Müller, L. Mora, E. Raymundo and J. D. Etchevers, Transport, sorption and degradation of atrazine in two clay soils from Mexico: Andosol and Vertisol, *Geoderma*, 2014, **232–234**, 628–639.
- 11 A. Oderinde and P. Diagboya, Sorption of competing heavy metals on Laterite, Federal Polytechnic Ilaro, *J. Pure Appl. Sci.*, 2023, **5**(1), 1–9.
- 12 L. Gaspar, L. Mabit, I. Lizaga and A. Navas, Lateral mobilization of soil carbon induced by runoff along karstic slopes, *J. Environ. Manage.*, 2020, **260**, 110091.
- 13 IPCC, [https://www.ipcc.ch/pdf/assessment-report/ar4/syr/ar4\\_syr\\_full\\_report.pdf](https://www.ipcc.ch/pdf/assessment-report/ar4/syr/ar4_syr_full_report.pdf), 2007, vol. 8.
- 14 UNFCCC, <https://unfccc.int/news/climate-change-is-an-increasing-threat-to-africa>, 2020.
- 15 B. A. Ogwang, M. H. Kabengwela, C. Dione and A. Kamga, *The State of Climate of Africa in 2017*, African Centre for



- Meteorological Applications for Development, Niamey, Niger, 2018.
- 16 P. Nimi, *Floods are Submerging Whole Houses in Nigeria. At Least 80 have Died Trying to Escape*, (accessed 12.10.2022, 2022).
  - 17 A. Cascais and A. S. Mohammad, *Africa: After the Drought Comes the Flood*, (accessed 22.09.2022, 2022).
  - 18 J. Omondi, *500 Killed, 1.4 Million Nigerians Displaced by Floods in 2022*, (accessed 12.10.2022, 2022).
  - 19 E. Tzanetou and H. Karasali, in *Pests, Weeds and Diseases in Agricultural Crop and Animal Husbandry Production*, ed. D. Kontogiannatos, A. Kourti and K. F. Mendes, IntechOpen, 2020, DOI: [10.5772/intechopen.93066](https://doi.org/10.5772/intechopen.93066).
  - 20 R. C. Pereira, P. R. Anizelli, E. Di Mauro, D. F. Valezi, A. C. S. da Costa, C. T. B. V. Zaia and D. A. M. Zaia, The effect of pH and ionic strength on the adsorption of glyphosate onto ferrihydrite, *Geochem. Trans.*, 2019, **20**, 3.
  - 21 P. N. Diagboya, J. Junck, S. O. Akpotu and R.-A. Düring, Isolation of aqueous pesticides on surface-functionalized SBA-15: glyphosate kinetics and detailed empirical insights for atrazine, *Environ. Sci.: Processes Impacts*, 2024, **26**, 323–333.
  - 22 O. K. Borggaard and A. L. Gimsing, Fate of glyphosate in soil and the possibility of leaching to ground and surface waters: a review, *Pest Manage. Sci.*, 2008, **64**, 441–456.
  - 23 W. A. Battaglin, M. T. Meyer, K. M. Kuivila and J. E. Dietze, Glyphosate and Its Degradation Product AMPA Occur Frequently and Widely in U.S. Soils, Surface Water, Groundwater, and Precipitation, *J. Am. Water Resour. Assoc.*, 2014, **50**, 275–290.
  - 24 E. Okada, D. Pérez, E. De Gerónimo, V. Aparicio, H. Massone and J. L. Costa, Non-point source pollution of glyphosate and AMPA in a rural basin from the southeast Pampas, Argentina, *Environ. Sci. Pollut. Res.*, 2018, **25**, 15120–15132.
  - 25 K. Guyton, D. Loomis, Y. Grosse, F. El Ghissassi, L. Benbrahim-Tallaa, N. Guha, C. Scocciati, H. Mattock and K. Straif, International Agency for Research on Cancer Monograph Working Group ILF. Carcinogenicity of tetrachlorvinphos, parathion, malathion, diazinon, and glyphosate, *Lancet Oncol.*, 2015, **16**, 490–491.
  - 26 M. J. Davoren and R. H. Schiestl, Glyphosate-based herbicides and cancer risk: a post-IARC decision review of potential mechanisms, policy and avenues of research, *Carcinogenesis*, 2018, **39**, 1207–1215.
  - 27 C. N. Albers, G. T. Banta, P. E. Hansen and O. S. Jacobsen, The influence of organic matter on sorption and fate of glyphosate in soil—comparing different soils and humic substances, *Environ. Pollut.*, 2009, **157**, 2865–2870.
  - 28 H. De Jonge, L. De Jonge, O. Jacobsen, T. Yamaguchi and P. Moldrup, Glyphosate sorption in soils of different pH and phosphorus content, *Soil Sci.*, 2001, **166**, 230–238.
  - 29 J. Dollinger, C. Dagès and M. Voltz, Glyphosate sorption to soils and sediments predicted by pedotransfer functions, *Environ. Chem. Lett.*, 2015, **13**, 293–307.
  - 30 S. Munira, A. Farenhorst, D. Flaten and C. Grant, Phosphate fertilizer impacts on glyphosate sorption by soil, *Chemosphere*, 2016, **153**, 471–477.
  - 31 I. A. Ololade, N. A. Oladoja, F. F. Oloye, F. Alomaja, D. D. Akerele, J. Iwaye and P. Aikpokpodion, Sorption of Glyphosate on Soil Components: The Roles of Metal Oxides and Organic Materials, *Soil Sediment Contam.: Int. J.*, 2014, **23**, 571–585.
  - 32 C. J. Meyer, F. Peter, J. K. Norsworthy and R. Beffa, Uptake, translocation, and metabolism of glyphosate, glufosinate, and dicamba mixtures in *Echinochloa crus-galli* and *Amaranthus palmeri*, *Pest Manage. Sci.*, 2020, **76**, 3078–3087.
  - 33 P. N. Diagboya, F. N. Mtunzi, K. O. Adebawale and B. I. Olu-Owolabi, Assessment of the effects of soil organic matter and iron oxides on the individual sorption of two polycyclic aromatic hydrocarbons, *Environ. Earth Sci.*, 2021, **80**, 227.
  - 34 P. N. Diagboya, B. I. Olu-Owolabi and K. O. Adebawale, Effects of time, soil organic matter, and iron oxides on the relative retention and redistribution of lead, cadmium, and copper on soils, *Environ. Sci. Pollut. Res. Int.*, 2015, **22**, 10331–10339.
  - 35 O. P. Mehra and M. L. Jackson, in *Clays and Clay Minerals*, ed. E. Ingerson, Pergamon, 2013, pp. 317–327, DOI: [10.1016/B978-0-08-009235-5.50026-7](https://doi.org/10.1016/B978-0-08-009235-5.50026-7).
  - 36 DIN-EN 15933, *Sludge, Treated Biowaste and Soil – Determination of pH*, DIN EN 15933:2012-11, 2012.
  - 37 DIN-EN-15936, *Sludge, treated biowaste, soil and waste – Determination of total organic carbon (TOC) by dry combustion*, DIN EN 15936:2012-11, 2012.
  - 38 DIN-ISO-11277, *Soil quality – Determination of Particle Size Distribution in Mineral Soil Material – Method by Sieving and Sedimentation*, DIN ISO 11277, 2002.
  - 39 DIN-EN-ISO-10693, *Soil Quality – Determination of Carbonate Content – Volumetric Method*, DIN EN ISO 10693:2014-06, 2014.
  - 40 DIN-EN-16174, *Sludge, Treated Biowaste and Soil - Digestion of Aqua Regia Soluble Fractions of Elements*, DIN EN 16174:2012-11, 2012.
  - 41 C. V. Waiman, M. J. Avena, M. Garrido, B. Fernández Band and G. P. Zanini, A simple and rapid spectrophotometric method to quantify the herbicide glyphosate in aqueous media. Application to adsorption isotherms on soils and goethite, *Geoderma*, 2012, **170**, 154–158.
  - 42 S. O. Duke, *Glyphosate: Environmental Fate and Impact*, Weed Science, 2020, vol. 68, pp. 201–207.
  - 43 A. J. Aubin and A. E. Smith, Extraction of [<sup>14</sup>C]glyphosate from Saskatchewan soils, *J. Agric. Food Chem.*, 1992, **40**, 1163–1165.
  - 44 I. I. Mokwenye, P. N. Diagboya, B. I. Oluowolabi, I. O. Anigbogu and H. I. Owamah, Immobilization of toxic metal cations on goethite-amended soils: a remediation strategy, *J. Appl. Sci. Environ. Manage.*, 2016, **20**, 436–443.
  - 45 B. I. Olu-Owolabi, P. N. Diagboya and K. O. Adebawale, Sorption and desorption of fluorene on five tropical soils from different climes, *Geoderma*, 2015, **239–240**, 179–185.
  - 46 S. Lagergren, Zur theorie der sogenannten adsorption gelöster stoffe. Kungliga Svenska Vetenskapsakademiens, *Handlingar*, 1898, **24**, 1–39.
  - 47 M. Haerifar and S. Azizian, Fractal-like kinetics for adsorption on heterogeneous solid surfaces, *J. Phys. Chem. C*, 2014, **118**, 1129–1134.



- 48 W. J. Weber and J. C. Morris, Kinetics of adsorption on carbon from solutions, *J. Sanit. Eng. Div., Am. Soc. Civ. Eng.*, 1963, **89**, 31–60.
- 49 P. N. Diagboya, A. Odagwe, H. H. Oyem, C. Omoruyi and E. Osabohien, Adsorptive decolorization of dyes in aqueous solution using magnetic sweet potato (*Ipomoea batatas* L.) peel waste, *RSC Sustainability*, 2024, **2**, 686–694.
- 50 E. B. AttahDaniel, F. M. Mtunzi, D. Wankasi, N. Ayawei, E. D. Dikio and P. N. Diagboya, Relative empirical evaluation of the aqueous sequestration of methylene blue using benzene-1,4-dicarboxylic acid-linked lanthanum and zinc metal organic frameworks, *Water, Air, Soil Pollut.*, 2022, **233**, 442.
- 51 S. O. Akpotu, P. N. Diagboya, I. A. Lawal, S. O. Sanni, A. Pholosi, F. M. Mtunzi and A. E. Ofomaja, Designer composite of montmorillonite-reduced graphene oxide-PEG polymer for water treatment: enrofloxacin sequestration and cost analysis, *Chem. Eng. J.*, 2023, **453**, 139771.
- 52 J. Junck, P. N. Diagboya, A. Peqini, M. Rohnke and R.-A. Düring, Mechanistic interpretation of the sorption of terbuthylazine pesticide onto aged microplastics, *Environ. Pollut.*, 2024, **345**, 123502.
- 53 T. Orcelli, E. di Mauro, A. Urbano, D. F. Valezi, A. C. S. da Costa, C. T. B. V. Zaia and D. A. M. Zaia, Study of Interaction Between Glyphosate and Goethite Using Several Methodologies: an Environmental Perspective, *Water, Air, Soil Pollut.*, 2018, **229**, 150.
- 54 B. I. Olu-Owolabi, P. N. Diagboya, F. M. Mtunzi and R.-A. Düring, Utilizing eco-friendly kaolinite-biochar composite adsorbent for removal of ivermectin in aqueous media, *J. Environ. Manage.*, 2021, **279C**, 111619.
- 55 B. I. Olu-Owolabi, P. N. Diagboya, F. M. Mtunzi, K. O. Adebawale and R.-A. Düring, Empirical aspects of an emerging agricultural pesticide contaminant retention on two sub-Saharan soils, *Gondwana Res.*, 2022, **105**, 311–319.
- 56 L. Yue, C. Ge, D. Feng, H. Yu, H. Deng and B. Fu, Adsorption-desorption behavior of atrazine on agricultural soils in China, *J. Environ. Sci.*, 2017, **57**, 180–189.
- 57 I. Langmuir, The constitution and fundamental properties of solids and liquids, *J. Am. Chem. Soc.*, 1916, **38**, 2221–2295.
- 58 H. M. F. Freundlich, Über die adsorption in lösungen, *Z. für Phys. Chem.*, 1906, **57A(57A)**, 385–470.
- 59 R. J. Umpleby, S. C. Baxter, Y. Chen, R. N. Shah and K. D. Shimizu, Characterization of Molecularly Imprinted Polymers with the Langmuir–Freundlich Isotherm, *Anal. Chem.*, 2001, **73**, 4584–4591.

